

OPTIMIZATION OF SOUND PULSE GENERATION FOR PHOTOACOUSTIC
SENSING APPLICATIONS

Markku Oksanen
Department of Physics
University of Helsinki
Siltavuorenpenger 20 D
SF00170 Helsinki, Finland

Junru Wu
Department of Physics
University of Vermont
Burlington, VT 05405, USA

INTRODUCTION

Photoacoustically generated sound pulses are currently used in various NDT, NDE and sensing applications, often because this method generates ultrasound without touching the sample. The generation mechanisms are relatively well known, including directional patterns, sound pressures and damage thresholds for the laser intensity. Our study addresses the optimal conditions for sound generation for sensing purposes in a liquid using a low power diode pumped Nd:YAG pulse laser.

THEORY

Photoacoustic generation mechanisms can be divided into three different regimes by the incident light intensity [1]. The thermoelastic regime is most useful because the theory of the generation mechanism for different source geometries is readily available [2,3,4] and the sound pressure spectral density can be easily calculated. Let us consider the situation in fig. 1.

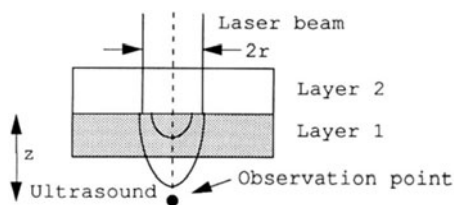


Fig.1 Photoacoustic source at an interface.

Here the laser power is absorbed at the interface of two solid layers. The temperature evolution at the interface can be evaluated for a harmonic heat source and used to solve the unidimensional elastic wave equation, giving the displacement amplitude of the elastic wave [5] which is used as the displacement amplitude of a piston source [6]. The diameter of the piston is taken to be the 1/e diameter of the beam at the interface. In our example the laser illumination has a pulse train type time dependency. It's spectra can be easily obtained [4] and taken in to account. Simple multiplication of the spectral contributions can be justified by a different treatment of the unidimensional theory [7]. Therefore the spectral content of the sound pressure, $p(\omega, z)$ on a line directly under the source at a distance z can be written as

$$p(\omega, z) = \omega \rho_1 v_1 t_1(\omega) t_2(z, \omega) t_3(\omega) \quad (1)$$

where $t_1(\omega)$, $t_2(\omega, z)$ and $t_3(\omega)$ are the photoacoustic conversion term, the contribution of the piston approximation and the spectral density of the pulse train respectively. They can be expressed as

$$t_1(\omega) = \frac{(1-i) h}{\sqrt{2\omega} \left(1 + \frac{\rho_1 v_1}{\rho_2 v_2}\right) (\kappa_1 a_1 + \kappa_2 a_2)} \left\{ \frac{z \lambda_1}{c_1 v_1 a_1^2} + \frac{(1-i)}{\sqrt{2\omega}} \left[\frac{\lambda_1}{c_1 a_1} + \frac{\lambda_2}{c_2 a_2} \right] \right\} \quad (2)$$

$$t_2(z, \omega) = 2 \sin \left\{ \frac{1}{2} \frac{\omega z}{v_1} \sqrt{1 + \left(\frac{r}{z}\right)^2} - 1 \right\} \quad (3)$$

$$t_3(\omega) = \tau \sqrt{\pi} \exp(\omega^2 t^2 / 4) \exp(i(N-1) \omega t / 2) \frac{\sin(N\omega t / 2)}{\sin(\omega t / 2)} \quad (4)$$

where $a = (\rho C_v \kappa)^{1/2}$, h = incident laser intensity, ρ = density, κ = thermal conductivity, ω = angular frequency, z = distance, λ = bulk modulus · volume thermal expansion coefficient, v = sound velocity, C_v = specific heat at constant volume, r = radius of the laser beam, N = number of pulses, τ = pulse length, and T = time between pulses. Subscript 1 refers to layer 1 and 2 to layer 2.

The parameters used were obtained from reference literature, with some difficulty in finding reliable figures for thermal parameters [8,9,10,11,12]. Other materials were also considered, for which theoretical figures are shown in table 1. The maximum sound pressure radiated to water from a Polyethylene-Polyethylene (PE-PE) sample with a geometry of fig.1 is scaled to be 1. Frequency is 4 MHz and distance from the source is 100 mm.

Table 1 Relative sound pressures.

Layer 1	Layer 2	Sound pressure ratio
Polyethylene (PE)	Polyethylene (PE)	1.0
Polyethylene	Air	0.1
Polystyrene	Polystyrene	2.0
Polystyrene	Air	0.1
Silicon rubber	Silicon Rubber	0.06
Polyethylene	Lucite	2.2

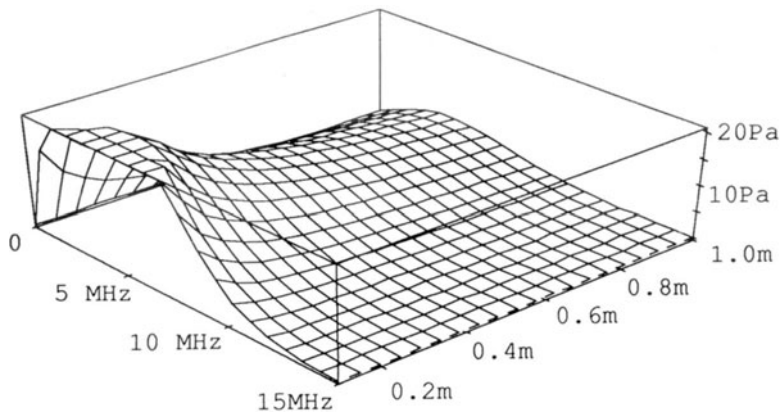


Fig.2 Sound pressure spectral density in water.

The theoretical spectral content of the signal can be plotted against frequency and distance from the source. The plot in fig. 2 shows the envelope of the comb-type spectral density of the sound pressure in water which is the same as the spectral density of only one pulse. Figure 2 corresponds to geometry in fig. 1 for a Lucite-PE-sample. The shape of the surface in fig.2 is determined mainly as follows: At low frequencies the piston source approximation dominates giving a decreasing behavior. At high frequencies the photoacoustic contribution and the laser pulse spectral density both contribute to the decreasing behavior. The $1/\text{distance}$ behavior is due to the piston approximation at all frequencies because that is the only term with distance dependence.

The material of layer 1 selected for our experimental study was polyethylene because it's acoustic impedance is very close to that of water and therefore offers 91% sound pressure transmission through the polyethylene-water interface. This ensures a clean pulse without reflections back and forth through the side of the sample which is facing the liquid. Plastics also have a favorable combination of thermal and elastic parameters for good generation efficiency. The transmission coefficient at PE water interface is taken into account also as a multiplier smaller than one at all frequencies.

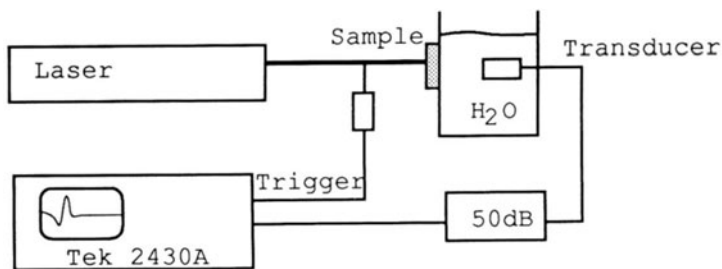


Fig.3 Measurement equipment.

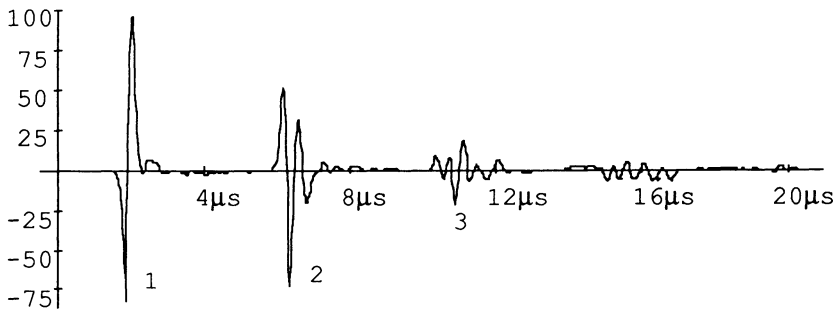
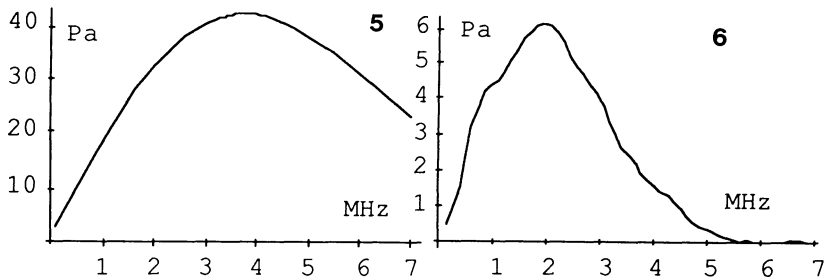


Fig.4 Detected pulses.

EXPERIMENT

The experimental equipment is described in fig. 3. The laser used was a laser diode pumped Nd:YAG-laser with a passive, LiF Q-switch. The power was 6 mW average, pulse duration 60 ns, and repetition frequency 15 kHz. The photoacoustic signal was detected with a commercial PZT-transducer. The detected waveform was stored and transferred to a computer for the spectral analysis. The thickness of both layers 1 and 2 in the experiment was 6.3 mm. The absorption takes place in a 20 layers of dyed 0.0013 mm thick polyethylene film. These layers are treated as a part of the PE layer of the sample in the theory.

Figure 4 shows the total detected pulse that includes reflections in the Lucite layer, which are labelled 2 and 3. Amplitude scale is arbitrary. We were interested in the pulse marked as 1. It's spectra can be seen in fig.6. The theoretical sound pressure-frequency curve in fig.5 shows more high frequencies than the measured spectral density. The detected signal is somewhat smaller than the predicted one. If the transducer frequency response is taken into account the maximum sound pressure agrees with the predicted, but the integrated spectral content is smaller and more concentrated on low frequencies as can be seen in fig.7.



Figs.5 and 6 Theoretical and measured spectral densities.

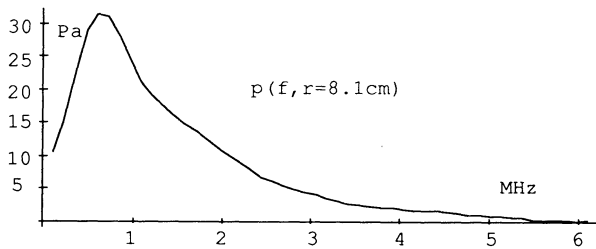


Fig.7 Pulse spectral density with transducer response.

This amplitude discrepancy can be explained with the uncertainty of the material parameters. The narrower spectra is due to the fact that the absorption takes place in a layer that is one tenth of a wavelength thick already at 7.6 MHz. This causes some cancellation of the higher frequencies in the on-axis waveform.

CONCLUSIONS

Very low power pulse lasers can be used to generate detectable ultrasound when the source geometry and material are chosen properly. It becomes clear that large, bulky lasers are not needed in photoacoustical applications, modern "MicroLasers" are powerful enough. Standard PZT-transducers can be used instead of expensive and tricky optical interferometers to detect the pulses.

ACKNOWLEDGEMENT

This work is supported by BFGoodrich Simmonds Precision Aircraft Systems, Vergennes VT.

REFERENCES

1. D.A.Hutchins, Can. J. Phys. 64, 1247 (1986)
2. L.M. Lyamshev, L.V Sedov, Akust. Zh 27, 5-29 (1981)
3. F.A. McDonald, Appl. Phys. Lett. 54 (16), (1989)
4. Y.H.Berthelot, J. Acoust.Soc. Am. 85 (3), (1989)
5. G.C. Wetsel, Jr. IEEE Trans. Vol UFFC-33, No. 5 (1986)
6. L.E.Kinsler, A.R.Frey, A.B.Coppens, J.P.Sanders, Fundamentals of Acoustics (J Wiley&Sons 1980) p.176
7. M.W. Sigrist, J. Appl. Phys. 60 (7) 1986
8. Cristopher Hall, Polymer Materials (Halsted Press, New York, 1980)
9. Thermophysical Properties of Matter (IFI/Plenum, 1970)
10. American Institute of Physics Handbook, 2rd Edition (Mc Graw-Hill, 1963)
11. J. Brandrup, E.H. Immergut, Polymer Handbook, 3rd Edition (John Wiley & Sons, New York, 1989)